ORIGINAL PAPER

Interference in the endplate nutritional pathway causes intervertebral disc degeneration in an immature porcine model

**Ran Kang · Haisheng Li · Steffen Ringgaard · Kresten Rickers ·
Haolin Sun · Muwan Chen · Lin Xie · Cody Bünger**

Abstract

Purpose Previous studies have shown that blocking the endplate nutritional pathway with bone cement did not result in obvious intervertebral disc degeneration (IDD) in mature animal models. However, there are very few comparable studies in immature animal models. As vertebroplasty currently is beginning to be applied in young, even biologically immature patients, it is important to investigate the effect of cement blocking at the endplate in an immature animal model.
Methods Two lumbar intervertebral discs in eight immature pigs were either blocked by cement in both endplate pathways or stabbed with a scalpel in the annulus fibrosus (AF) as a positive control, and with a third disc remaining intact as a normal control. Magnetic resonance imaging (MRI) and histology study were performed.
Results After three months, the cement-blocked discs exhibited severe IDD, with the percentage of disc-height index (DHI), nucleus pulposus (NP) area, and NP T2 value significantly lower than the normal control. These IDD changes were histologically confirmed. Post-contrast MRI showed diseased nutritional diffusion patterns in the cement-blocked discs. Moreover, the degenerative changes of the cement-blocked discs exceeded those of the injured AF positive controls.

Conclusions The endplate nutritional pathway was interfered with and diseased after three months of bone cement intervention in an immature porcine model. Severe interference in the endplate nutritional pathway in an immature porcine model caused IDD. These findings also draw attention to the fact that interference in endplate nutritional pathways in immature or young patients may affect the vitality of adjacent discs.

Keywords Endplate nutritional pathway · Intervertebral disc degeneration · Vertebroplasty · Bone cement · MRI · Immature porcine model

R. Kang (✉) · H. Li · K. Rickers · H. Sun · M. Chen · C. Bünger
Orthopaedic Research Laboratory, Aarhus University,
Building 1A, Noerrebrogade 44, 8000 Aarhus C, Denmark
e-mail: kang.ran@ki.au.dk

S. Ringgaard
The MR Research Centre, Aarhus University Hospital, Skejby,
Aarhus C 8000, Denmark

R. Kang · L. Xie
Department of Orthopedic Surgery, Jiangsu Province Hospital on
Integration of Chinese and Western Medicine,
Nanjing 210028, China

Introduction

Intervertebral disc degeneration (IDD) is characterized by impairment of disc structure and loss of proteoglycan and water content in extracellular matrix (ECM) [1, 2]. IDD changes start in childhood and may cause biomechanical disc dysfunction and low back pain symptoms later in life [3]. While the pathology of IDD is not fully understood, insufficient nutritional supply to the disc has been proposed as a possible initiator of IDD [4].

Intervertebral discs are the largest avascular organs in humans; they obtain nutrition from adjacent vertebral bodies by means of diffusion through the endplate [5]. In acute animal studies (studies completed in the course of a few hours), blockage of this pathway resulted in an obvious decrease in diffusion transportation to the nucleus pulposus (NP) [6, 7]; the endplate pathway was found to be the main nutritional route in comparison to the other annulus fibrosus (AF) pathways [6]. In in-vitro studies, an insufficient nutritional environment leads to a significant reduction in disc matrix gene expression and loss of ECM and may even cause disc cell death [8, 9]. In humans, association between IDD and decreased blood supply in the adjacent vertebral body has also

been found [10]. These findings suggest that IDD arises from the altered nutrition supply.

Blocking the endplate nutritional pathway with bone cement for a certain period (several months to 1.5 years) produced no obvious IDD in several adult animal models [11–13]. Interfering in the endplate pathway does not seem to affect the health of adjacent discs in mature animal models. However, there have been far fewer studies in immature animal models. As vertebroplasty is currently beginning to be employed in younger patients, including a biologically immature 16-year-old [14], and is no longer limited to older patients, it is vitally important to investigate the effect of interference in the endplate nutritional pathway in an immature animal model.

Materials and methods

Surgical procedure

Eight Danish landrace immature pigs were used for the study (all females, three months old, weight approximately 35 kg). The experimental procedures were approved by the Danish Animal Welfare Committee. Under general anaesthesia, the pigs were placed in supine position. After routine sterilization and draping, a left-sided retroperitoneal approach was used to expose the lumbar spine. The psoas muscle was gently detached from the intervertebral discs, and care was taken to keep the segmental artery intact. Due to variability in the number of lumbar vertebrae in pigs (five, six or seven), the disc level was selected with reference to the lumbosacral junction [15]. This reference level was set as disc 7 and the others cranial to this level were then marked in descending order to disc 0.

Similarly to the design of a previous study [11], disc 0 was kept intact and served as a normal control, and disc 4 or disc 5 was interfered with either by scalpel or cement as follows. One disc was stabbed with a no. 23 scalpel at the left anterolateral part at a depth of 6 mm (just reaching the NP; in a pilot study, we measured the AF width to be about 6 mm) as a positive control [15, 16]. In the other disc, a slice defect was created in the vertebral body both caudally and cranially to the disc by drilling and curetting. The slices were made parallel and close to the endplates without violating the integrity of the endplates. Using a custom-made injection gun, the defects were then filled with bone cement (polymethylmethacrylate [PMMA] 64.4 %, benzoyl peroxide 0.6 %, barium sulfate 35 %, William Cook Europe ApS) and checked by means of fluoroscopy to ensure that there was no cement leakage into the canal or disc. Hemostasis was secured and the abdomen was closed in layers. The pigs were housed in separate boxes and fed a standardized food recipe.

Magnetic resonance imaging (MRI) procedure and evaluation

MRI was performed under general anesthesia on a clinical Philips Achieva 1.5-T scanner (Philips Healthcare, Best, Netherlands). Before surgery and at termination, sagittal T1- and T2-weighted, T2-weighted 3D scan, and a sagittal T2 mapping scan (multi-echo spin echo; matrix 248 × 248; field of view 300 × 300 mm; repetition time 1.0 second; eight echoes with echo time 15–120 milli-seconds; two excitations) were performed. At termination, after manual injection of 0.3 mmol/kg gadolinium (OMNISCAN™, Amersham Health AS, Oslo), post-contrast T1-weighted images were obtained at intervals of 0.5, five, and ten minutes and then every ten minutes for a total of 110 minutes. All images were analysed using a custom programmed software written by one of the authors (SR).

The blocking area was defined as the percentage of maximum cement area (% block-area) in the vertebral body parallel to the endplate in T2-weighted 3D images of both sides. Degree of IDD was assessed as follows [17]: Severe (score= 3): evident reduction in the NP area, decrease in NP signal intensity (SI) along with collapse of the AF; Mild (score=2): moderate reduction in the NP area, less severe decrease in NP SI, collapse of the AF frequently found; Normal (score=1): no changes in SI and disc morphology. The change of disc height index (DHI) was expressed as percentage of DHI (% DHI) (%DHI=postoperative DHI / preoperative DHI × 100) as previously described in the literature [18–20]. The change in NP area was calculated as percentage of NP area (% NP-area) in the middle axial position of the disc on T2-weighted 3D images (%NP–area=postoperative NP area / preoperative NP area × 100). T2 value within the NP was calculated by means of a T2 decay equation [19]. Contrast enhancement within the NP was calculated as percentage of contrast enhancement (% CE) (% CE=(SI_{post} − SI_{pre}) / SI_{pre} × 100). Time-intensity curves were drawn according to % CE and each time point [21].

Histology

The animals' disc segments were removed at termination and fixed with 70 % ethanol for seven days, dehydrated in a series of ethanol concentrations, and embedded in methyl methacrylate. Sections of 7 μm were stained with hematoxylin-eosin (HE), picrosirius red for collagen and toluidine blue for proteoglycan. They were then examined using a photomicroscope (Olympus, Tokyo, Japan).

Statistical analysis

The data are expressed as the mean±standard deviation. Data of % DHI, % NP-area, and NP T2 value were compared using

Table 1 Disc location, cement blocking area, and intervertebral disc degeneration (IDD) degree after three months of different interventions

Number	Cement			Scalpel		Normal	
	Disc	Blocking area (%)	IDD degree	Disc	IDD degree	Disc	IDD degree
1	4	27.09	2	5	2	0	1
2	4	35.01	3	5	1	0	1
3	5	30.32	3	6	2	0	1
4	4	32.31	3	5	2	0	1
5	5	46.20	3	4	2	0	1
6	5	50.56	3	4	2	0	1
7	5	50.93	3	4	2	0	1
Average		38.92±10.05	2.86±0.38		1.86±0.38		1.00

one way-ANOVA analysis between the different interventions. Significance level was defined as P less than 0.05.

Results

All eight pigs tolerated the surgical procedure well and were neurologically intact. One pig had an incisional hernia postoperatively and was immediately euthanised. The other seven pigs continued to the end of the three-month observation period.

The location of each intervention, cement blocking area, and IDD degree are listed in Table 1. In general, these cement-blocked discs had severe IDD, with obviously diminished disc height and NP area. Moreover, the color-coded T2 maps showed lower NP T2 value in the cement-blocked discs and scalpel-stabbed discs, as compared to the normal controls (Fig. 1). The % DHI of 70.59 ± 13.09 %, % NP-area of 53.25 ± 11.05 %, and the NP T2 value of 188.43 ± 75.66 ms in cement-blocked discs were significantly lower than those of the normal controls ($P=0.003$, $P<0.001$, $P<0.001$, respectively). The scalpel-stabbed discs had less severe changes in these three parameters (Fig. 2).
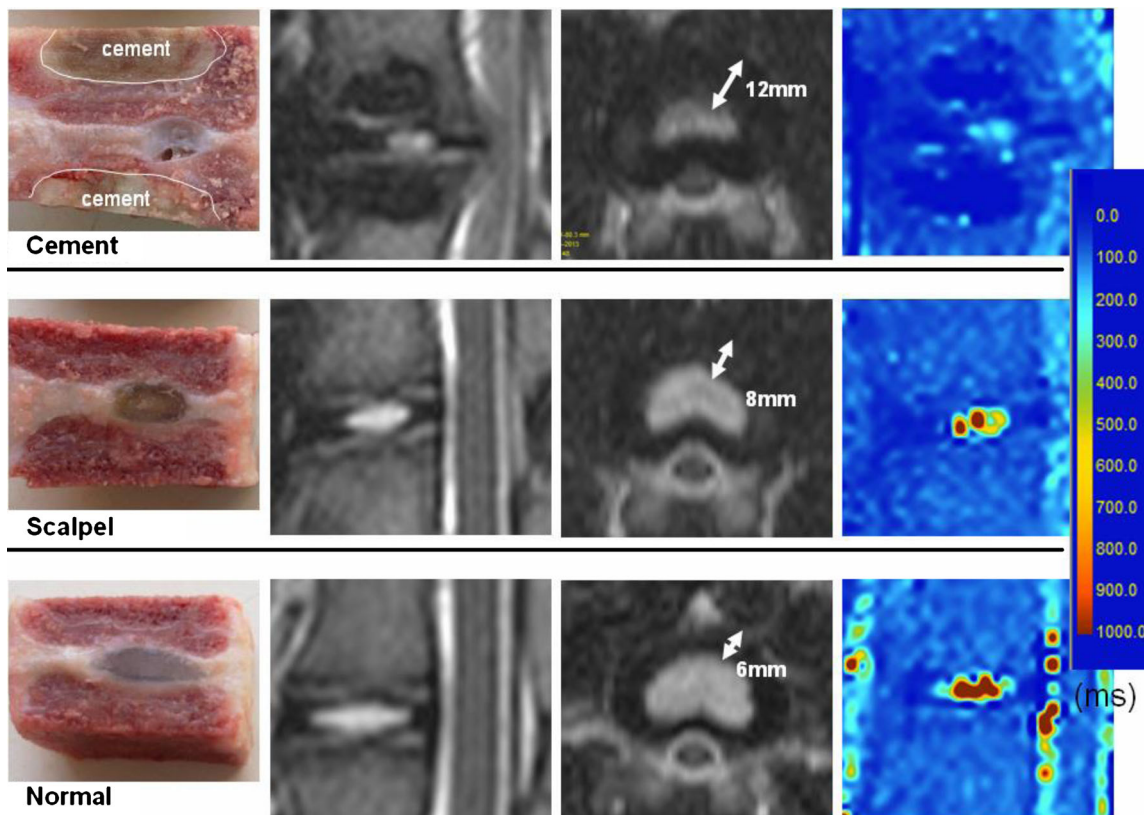

Fig. 1 The specimens, MRI T2-weighted sagittal and axial images, and color-coded MRI T2 mapping images of discs after three months of intervention. The nucleus pulposus (NP) signal, disc height, NP area, and NP T2 value obviously diminished in cement-blocked disc (the first row)

Fig. 2 The % DHI, % nucleus pulposus (NP)-area, and NP T2 value of discs in different interventions. * Indicates significant difference between the intervened discs and the normal controls, *P*<0.01
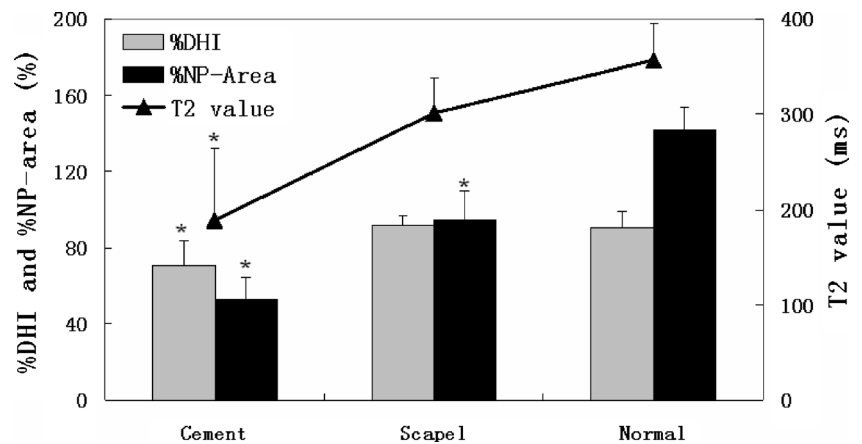
In post-contrast MRI images (Fig. 3), the enhancement of normal discs was seen as uniform enhancement bands parallel to the endplate and slowly moving towards the centre as time passed. In the cement-blocked discs, there were two different patterns. One pattern in five discs had enhancement bands with small pooling of dye at the edge. Another pattern in two discs had no visualized diffusion bands but rapid extensive pooling of the dye in the center. The corresponding time-intensity curve (Fig. 4) showed decreased diffusion or very early peak enhancement of the two patterns in cement-blocked discs, as compared to normal controls. No obvious diffusion difference was found between scalpel-stabbed discs and the normal discs.

Histological images of HE staining are shown in (Fig. 5a, d, g). In the cement-blocked discs, degenerative changes were obvious, including loss of NP cells, bulging and collapse of AF, and loss of the normal boundary between AF and NP. In the scalpel-stabbed discs, changes were mainly in the AF tissue with derangement of collagen fibers. No changes were detected in the normal controls. We continued by applying specific

staining for the disc ECM components of collagen and proteoglycan (overview in Fig. 5b, e, h, c, f, i). The cement-blocked discs showed collapse of AF (Fig. 5i), a thin endplate with little ECM (Fig. 5k), and very few NP ECM (Fig. 5l). The scalpel-stabbed discs showed disorganized AF as well as ECM loss in endplates in NP (Fig. 5m–o). The normal controls were healthy with regular fibrous lamellae, uniformly thick endplate, and with plentiful amounts of ECM in the NP (Fig. 5p–r).

Discussion

IDD is multifactorial. Abnormal loading, acute injury, even certain medical treatments such as stiff spinal fixation with resultant adjacent disc degeneration, can accelerate IDD [22]. As bone cement is widely used in vertebroplasty or balloon kyphoplasty, procedures that are performed in locations close to the endplates, concerns about the possible role of cement in interference in endplate nutritional pathways are reasonable. In our study, we demonstrated that bone cement blockage
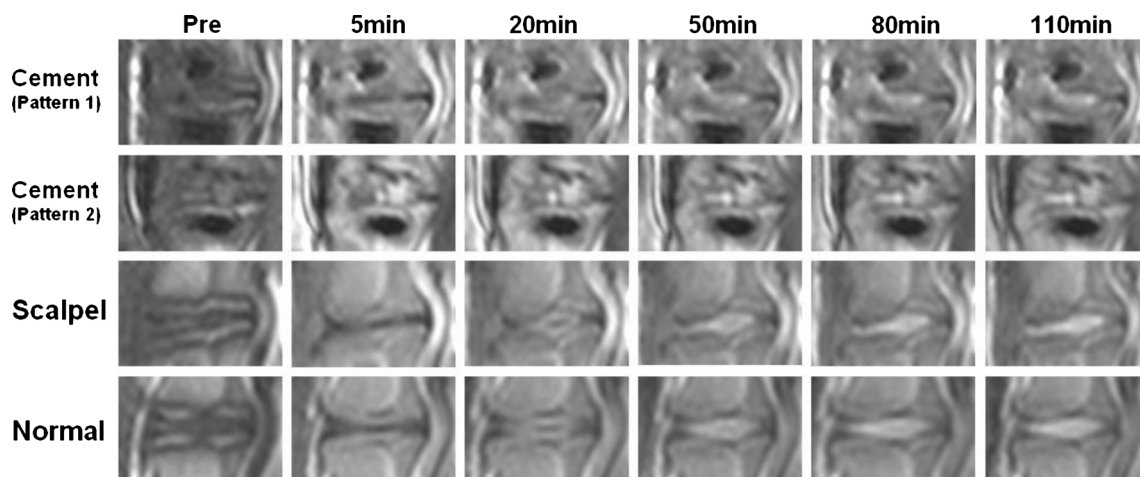

Fig. 3 The serial T1-weighted post-contrast MRI images of discs in different interventions. In cement-blocked disc, pattern 1 had enhancement bands parallel to the endplate, with small pooling of dye at the edge of bands; pattern 2 had no visualized diffusion bands but rapid extensive pooling of the dye in the center at five minutes. In scalpel-stabbed and normal discs, uniform enhancement bands parallel to the endplate slowly moved towards the centre as time passed
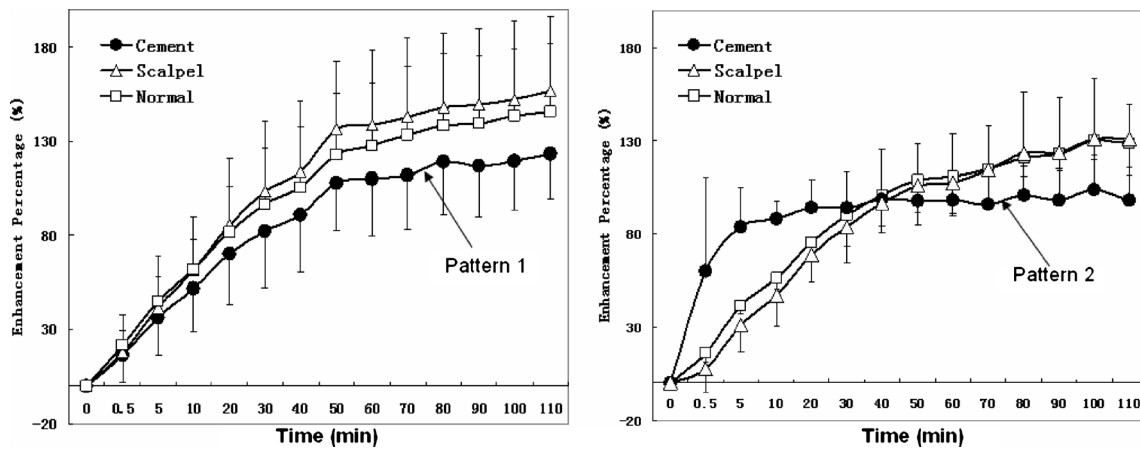
Fig. 4 Time-intensity curve. *Left*, pattern 1 of cement-blocked discs (*n*=5) had enhancement less than normal discs; *Right*, pattern 2 of cement-blocked discs (n=2) had very early peak enhancement as compared to normal discs

interference in endplate nutritional pathways caused IDD in an immature porcine model.

In a clinical setting, vertebroplasty treatment is mainly employed in older patients, whose discs are already aged or degenerated. Whether or not employing this method in young or even immature patients with much healthier discs is prudent requires further investigation. In our experiment, we found obvious adjacent IDD in an immature porcine model in

Fig. 5 Histological images of discs in different interventions. (**a-i**) Overview of the discs in different histological staining. (**j–r**) Images with higher magnification. Picosirius red staining viewed under polarized light: (**j**) irregular and collapse AF (*arrow*); (**m**) irregular fibrous lamellae (*arrow*); (**p**) regular fibrous lamellae. Toluidine blue staining: (**k**) disorganized endplate with loss matrix (*arrow*); (**n**) focal thinning of the EP (*arrow*); (**q**) uniformly thick EP with organized ECM; (**l**) very few matrix in NP (*arrow*); (**o**) matrix loss in NP; (**r**) normal matrix in NP
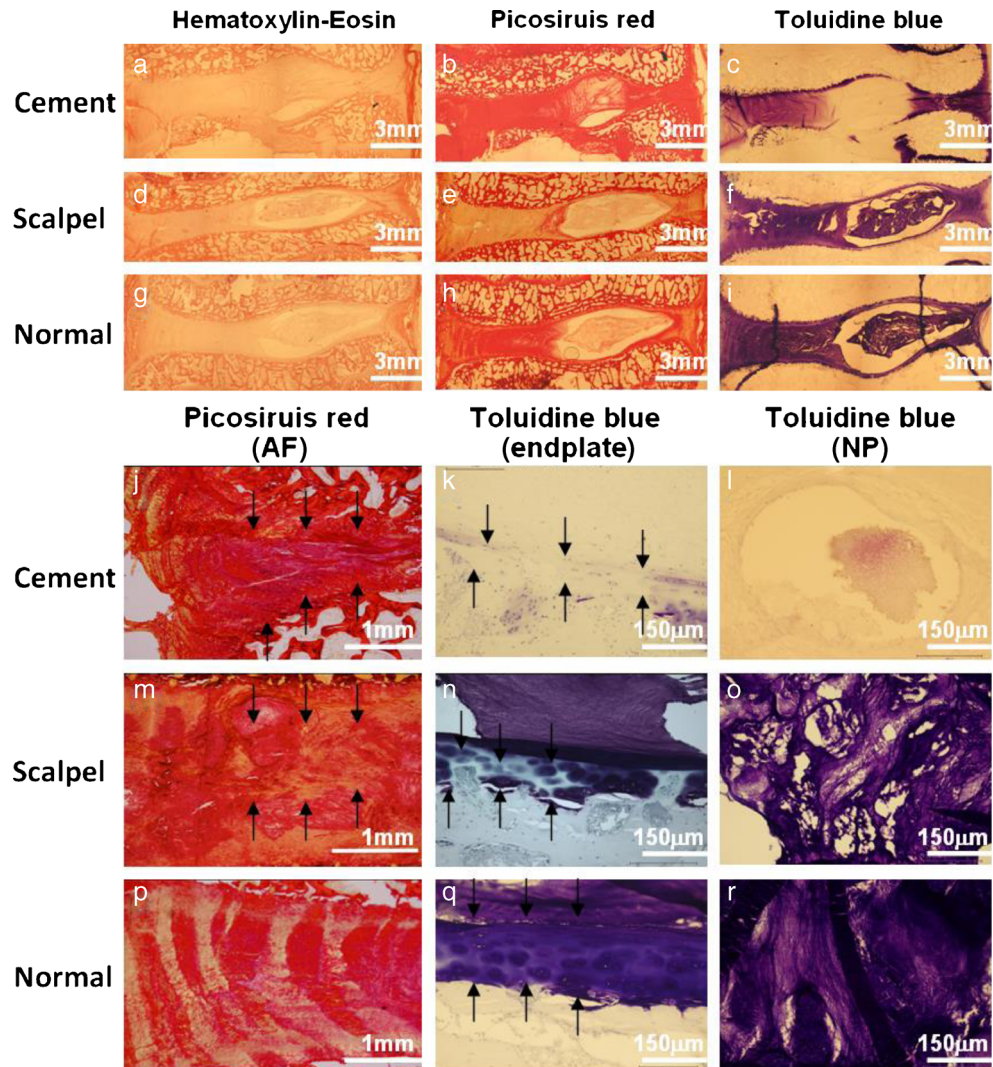
conjunction with blockage of the endplate by bone cement. Previously, similar studies in mature animal models did not find IDD. After unilaterally blocking endplates in an adult dog model, Hutton, et al. [12] did not find any visible IDD, but found slightly abnormal histological changes. After unilaterally blocking, and even breaking, endplates in a mature goat model, Verlaan et al.[13] did not find histological evidence for IDD. This negative result might be attributable to the fact that the other side of the endplate pathway continued to provide adequate nutrition. Krebs et al. [11], after injecting bone cement covering 80 % of the length of both sides of the endplates in the sagittal plane in a 7.2-year-old ewe model, found no significant IDD either. This might be because the cancellous bone mixed into the bone cement continuously provides a degree of blood supply for discs. Moreover, in the same study, new bone formation around the cement indicated that in the gap of bone and cement, a nutritional supply still existed. While these studies provided knowledge in relation to nutritional conditions, they did not provide further post-intervention data.

In our experiment, we scraped the cancellous bone near the endplate and fully filled the void by injecting bone cement in a manner similar to balloon kyphoplasty. In this way, we thoroughly blocked both endplate pathways. This was also similar to the method reported in previous acute in vivo studies of inserting a foil close to and parallel with the endplate to block the endplate nutritional route, resulting in significantly decreased diffusion to the disc [6, 7]. In our study, the relatively complete blockage on both sides of the endplate pathway, with no gap inside the cement, may be more likely to cause IDD. Furthermore, discs from our immature porcine model were still in the developing stage and probably demanded more nutrition in comparison to mature animal models. Previously, Ibrahim et al. [23] found that diffusion through the endplate was significantly greater in immature animals compared to mature animals. Greater nutritional demands may make these discs more vulnerable to changes in nutrition supply, possibly leading to more positive results. Previous studies reporting that injury to the endplates results in IDD in an immature model [17], but not in a mature animal model [13], supports to some extent the notion that the immature model is sensitive to interference in the nutritional pathway.

IDD is commonly characterized by MRI with reduced signal strength in T2-weighted images in NP, collapse of the annulus, and reduced disc height [24]. In our experiment, these characteristics were clearly observed in the cement-blocked discs. We used MRI T2 mapping to analyse changes in disc matrix composition. Compared to the normal controls, NP T2 values significantly declined in the cement-blocked discs. This result was consistent with previous studies [2, 3] where the lower T2 value reflects more severe disc degeneration, and reductions in T2 values indicate reduction of ECM and water content. We were able to conclude that the cement-blocked discs were pathologically degenerated. Diffusion study offers a powerful means of understanding the circumstances of disc nutrition. As Rajasekaran et al. have previously described, the pattern with decreased diffusion indicates decreased nutrition supply to the disc, while the pattern with vascularization phenomenon indicates very severe IDD with totally abnormal diffusion [4, 21, 25]; both of these indicated that the endplate nutritional pathway was interfered with and diseased as a result of bone cement intervention.

Histological examination showed obvious IDD changes including the collapse of AF, ECM loss in the NP, and endplate lesions in both the cement-blocked discs and scalpel-stabbed discs. These results were consistent with the MRI findings, and confirmed that discs had degenerated after cement interference in endplate nutritional pathways.

The limitation of the present study is the thermal effect of bone cement, which may cause tissue necrosis, which in turn may also more or less contribute to the positive findings. Because previous similar studies using PMMA cement in adult animals did not cause obvious abnormal histological changes [11–13], and the bone cement in our study was located at some distance from the endplate (Fig. 1), this effect might be minimal but can not be absolutely excluded.

Conclusions

In an immature porcine model, endplate nutritional pathways were interfered with and diseased after three months of bone cement intervention. Severe interference in endplate nutritional pathways in an immature porcine model caused IDD. Although such serious blocking is rarely seen in connection with vertebroplasty, the results of this experiment also draw attention to the fact that interference in endplate nutritional pathways in immature or young patients may affect the vitality of adjacent discs.

Conflict of interest The authors declare that they have no conflict of interest.

References

1. Patel KP, Sandy JD, Akeda K, Miyamoto K, Chujo T, An HS, Masuda K (2007) Aggrecanases and aggrecanase-generated fragments in the human intervertebral disc at early and advanced stages of disc degeneration. Spine 32(23):2596–2603. doi:10.1097/BRS.0b013e318158cb85
2. Takashima H, Takebayashi T, Yoshimoto M, Terashima Y, Tsuda H, Ida K, Yamashita T (2012) Correlation between T2 relaxation time

and intervertebral disk degeneration. Skelet Radiol 41(2):163–167. doi:10.1007/s00256-011-1144-0

3. Beattie PF (2008) Current understanding of lumbar intervertebral disc degeneration: a review with emphasis upon etiology, pathophysiology, and lumbar magnetic resonance imaging findings. J Orthop Sports Phys Ther 38(6):329–340. doi:10.2519/jospt.2008.2768

4. Rajasekaran S, Naresh-Babu J, Murugan S (2007) Review of postcontrast MRI studies on diffusion of human lumbar discs. J Magnetic Resonance Imaging JMRI 25(2):410–418. doi:10.1002/jmri.20853

5. Grunhagen T, Shirazi-Adl A, Fairbank JC, Urban JP (2011) Intervertebral disk nutrition: a review of factors influencing concentrations of nutrients and metabolites. Orthop Clin N Am 42(4):465–477. doi:10.1016/j.ocl.2011.07.010, vii

6. Ogata K, Whiteside LA (1981) 1980 Volvo award winner in basic science. Nutritional pathways of the intervertebral disc. An experimental study using hydrogen washout technique. Spine 6(3):211–216

7. van der Werf M, Lezuo P, Maissen O, van Donkelaar CC, Ito K (2007) Inhibition of vertebral endplate perfusion results in decreased intervertebral disc intranuclear diffusive transport. J Anat 211(6):769–774. doi:10.1111/j.1469-7580.2007.00816.x

8. Rinkler C, Heuer F, Pedro MT, Mauer UM, Ignatius A, Neidlinger-Wilke C (2010) Influence of low glucose supply on the regulation of gene expression by nucleus pulposus cells and their responsiveness to mechanical loading. J Neurosurg Spine 13(4):535–542. doi:10.3171/2010.4.SPINE09713

9. Johnson WE, Stephan S, Roberts S (2008) The influence of serum, glucose and oxygen on intervertebral disc cell growth in vitro: implications for degenerative disc disease. Arthr Res Ther 10(2):R46. doi:10.1186/ar2405

10. Liu YJ, Huang GS, Juan CJ, Yao MS, Ho WP, Chan WP (2009) Intervertebral disk degeneration related to reduced vertebral marrow perfusion at dynamic contrast-enhanced MRI. AJR Am J Roentgenol 192(4):974–979. doi:10.2214/AJR.08.1597

11. Krebs J, Ferguson SJ, Goss BG, Stauffer E, Ettinger L, Aebli N (2012) Effect of vertebral cement augmentation with polymethylmethacrylate on intervertebral disc and bone tissue. J Biomed Mater Res B Appl Biomater 100(3):660–667. doi:10.1002/jbm.b.31990

12. Hutton WC, Murakami H, Li J, Elmer WA, Yoon ST, Minamide A, Akamaru T, Tomita K (2004) The effect of blocking a nutritional pathway to the intervertebral disc in the dog model. J Spinal DisordTech 17(1):53–63

13. Verlaan JJ, Oner FC, Slootweg PJ, Verbout AJ, Dhert WJ (2004) Histologic changes after vertebroplasty. J Bone Joint Surg Am Vol 86-A(6):1230–1238

14. Rahamimov N, Mulla H, Shani A, Freiman S (2012) Percutaneous augmented instrumentation of unstable thoracolumbar burst fractures. Eur Spine J 21(5):850–854. doi:10.1007/s00586-011-2106-x

15. Yoon SH, Miyazaki M, Hong SW, Tow B, Morishita Y, Hu M, Ahn SJ, Wang JC (2008) A porcine model of intervertebral disc degeneration induced by annular injury characterized with magnetic resonance imaging and histopathological findings. Laboratory investigation. J Neurosurg Spine 8(5):450–457. doi:10.3171/SPI/2008/8/5/450

16. Bendtsen M, Bunger CE, Zou X, Foldager C, Jorgensen HS (2011) Autologous stem cell therapy maintains vertebral blood flow and contrast diffusion through the endplate in experimental intervertebral disc degeneration. Spine 36(6):E373–E379. doi:10.1097/BRS.0b013e3181dce34c

17. Cinotti G, Della Rocca C, Romeo S, Vittur F, Toffanin R, Trasimeni G (2005) Degenerative changes of porcine intervertebral disc induced by vertebral endplate injuries. Spine 30(2):174–180

18. Masuda K, Imai Y, Okuma M, Muehleman C, Nakagawa K, Akeda K, Thonar E, Andersson G, An HS (2006) Osteogenic protein-1 injection into a degenerated disc induces the restoration of disc height and structural changes in the rabbit anular puncture model. Spine 31(7):742–754. doi:10.1097/01.brs.0000206358.66412.7b

19. Obata S, Akeda K, Imanishi T, Masuda K, Bae W, Morimoto R, Asanuma Y, Kasai Y, Uchida A, Sudo A (2012) Effect of autologous platelet-rich plasma-releasate on intervertebral disc degeneration in the rabbit anular puncture model: a preclinical study. Arthrit Res Ther 14(6):R241. doi:10.1186/ar4084

20. Masuda K, Aota Y, Muehleman C, Imai Y, Okuma M, Thonar EJ, Andersson GB, An HS (2005) A novel rabbit model of mild, reproducible disc degeneration by an anulus needle puncture: correlation between the degree of disc injury and radiological and histological appearances of disc degeneration. Spine 30(1):5–14

21. Rajasekaran S, Babu JN, Arun R, Armstrong BR, Shetty AP, Murugan S (2004) ISSLS prize winner: A study of diffusion in human lumbar discs: a serial magnetic resonance imaging study documenting the influence of the endplate on diffusion in normal and degenerate discs. Spine 29(23):2654–2667

22. Videbaek TS, Egund N, Christensen FB, Grethe Jurik A, Bunger CE (2010) Adjacent segment degeneration after lumbar spinal fusion: the impact of anterior column support: a randomized clinical trial with an eight- to thirteen-year magnetic resonance imaging follow-up. Spine 35(22):1955–1964. doi:10.1097/BRS.0b013e3181e57269

23. Ibrahim MA, Haughton VM, Hyde JS (1995) Effect of disk maturation on diffusion of low-molecular-weight gadolinium complexes: an experimental study in rabbits. AJNR Am J Neuroradiol 16(6):1307–1311

24. Pfirrmann CW, Metzdorf A, Zanetti M, Hodler J, Boos N (2001) Magnetic resonance classification of lumbar intervertebral disc degeneration. Spine 26(17):1873–1878

25. Rajasekaran S, Venkatadass K, Naresh Babu J, Ganesh K, Shetty AP (2008) Pharmacological enhancement of disc diffusion and differentiation of healthy, ageing and degenerated discs: results from in-vivo serial post-contrast MRI studies in 365 human lumbar discs. Eur Spine J 17(5):626–643. doi:10.1007/s00586-008-0645-6